scientific reports

Check for updates

OPEN

Real-time imaging of blood coagulation and angiogenesis during development in a zebrafish model of type I antithrombin deficiency

Yuta Imai[1], Satoru Ozaki[1], Taiki Noda[1], Isao Kobayashi[2], Kayo Sugitani[1], Satomi Kasashima[1], Eriko Morishita[1,3]✉ & Yuhei Araiso[1]✉

Severe type I antithrombin (AT) deficiency is considered to cause embryonic lethality. Although several pathological analyses using mice or zebrafish have been attempted, the previous studies did not unveil the detailed mechanism leading to lethality in the early developmental stage. In order to solve this problem, we established type I AT deficient zebrafish by the CRISPR/Cas9 system into *Tg(gata1:dsRed)* and *Tg(fli1a:GFP)* lines, so that we could conduct real-time imaging of thrombosis and angiogenesis using fluorescence stereo zoom microscopy. The established zebrafish AT (zAT) mutants harbored frameshift mutations which resulted to be type I AT deficient, unable to secrete zAT protein into blood. Both heterozygous ($zAT^{+/-}$) and homozygous ($zAT^{-/-}$) mutants showed reduced survival rate and diverse thrombosis up to 9 days post fertilization. In addition, blood vessel formation was delayed at 30 hpf in $zAT^{-/-}$, which was recovered normally by 5 dpf and had little effect on survival. Notably, we analyzed the differences in gene expression profiles under AT-depleted conditions by real-time quantitative PCR, and $zAT^{-/-}$ juvenile zebrafish showed increased *PLG* gene expression and decreased *F2* gene expression. Our in vivo study revealed the effects of AT deficiency on embryos during development from the aspects of coagulation and vascular formation.

Keywords Antithrombin deficiency, Zebrafish, Genome editing, Thrombosis, Angiogenesis

Abbreviations

AT	Antithrombin
zAT	Zebrafish antithrombin
gRNA	Guide RNA
IPTG	Isopropyl β-D-thiogalactoside
dpf	Days post-fertilization
PFV	Pectoral fin vessel
PCV	Posterior cardinal vein
ISVs	Intersegmental vessels
Hpf	Hour-post fertilization
DLAVs	Dorsal longitudinal anastomotic vessels
NMD	Nonsense-mediated mRNA decay

Antithrombin (AT) in human is a single-chain protein composed of 464 amino acids, encoded by the *SERPINC1* gene, that is secreted into the blood as a mature protein of 432 amino acids after the cleavage of a 32 amino acid signal sequence[1]. Secreted AT plays a critical role in regulating blood coagulation by inhibiting various blood coagulation factors, including thrombin and coagulation factor X[1–3]. In addition, previous studies have

[1]Department of Clinical Laboratory Science, Division of Health Sciences, Graduate School of Medical Sciences, Kanazawa University, 5-11-80 Kodatsuno, Kanazawa, Ishikawa 920-0942, Japan. [2]Faculty of Biological Science and Technology, Institute of Science and Engineering, Kanazawa University, Kanazawa, Ishikawa, Japan. [3]Department of Hematology, Kanazawa University Hospital, Kanazawa, Ishikawa, Japan. ✉email: eriko86@staff.kanazawa-u.ac.jp; araiso@staff.kanazawa-u.ac.jp

demonstrated that various forms of AT, such as proteinase-cleaved AT, prelatent AT, and latent AT, possess anti-angiogenic properties. In some cases, these properties have been observed to induce tumor regression by inhibiting angiogenesis in chick embryo and mouse models[4–6].

Hereditary AT deficiency arises from mutations in the *SERPINC1* gene, elevating the risk of venous thrombosis by 5- to 16-fold[7,8]. This condition is categorized into two types: type I and type II. Type I is characterized by reducing levels of AT antigen in the blood due to impaired secretion of the AT protein, whereas in type II, AT antigen levels are normal, but its activity is reduced[9]. The abnormal variants of the *SERPINC1* gene that cause type I AT deficiency display a heterogeneous variant profile, with most frameshift involving small deletions or insertions linked to this type[10,11]. Conversely, compound heterozygous variants of the *SERPINC1* gene have been reported to cause embryonic lethality in humans[12]. In mice, severe AT deficiency manifests as fibrin deposition in fetal heart and liver tissues, accompanied by paradoxical subcutaneous bleeding due to consumptive coagulopathy[13].

Zebrafish (*Danio rerio*), classified as a teleost fish, possess highly conserved orthologs of various blood coagulation and anticoagulation factors, making them well suited for use in thrombotic studies involving AT, coagulation factor X, and fibrinogen[14–17]. Furthermore, the transparent nature of both fertilized eggs and fry facilitates observations of the circulatory system by fluorescent labeling, and their high reproductive capacity makes them useful for high-throughput pathological analysis[18,19]. A previous study utilized a zinc finger nuclease technique to establish a homozygous AT-deficient zebrafish line, which exhibited intracardiac thrombosis and adult mortality[14]. However, the detailed pathogenesis of zebrafish development associated with severe zebrafish AT (zAT) deficiency remains to be elucidated. In this study, we established heterozygous ($zAT^{+/-}$) and homozygous ($zAT^{-/-}$) mutant zebrafish lines using the CRISPR/Cas9 system in transgenic zebrafish fluorescently labeled with red blood cells and vascular endothelial cells. This technology allowed for the real-time visualization of thrombus formation, thereby enabling investigation of the effects of hereditary AT deficiency on zebrafish development.

Results

Introduction of frameshift mutation into the zebrafish *SERPINC1* gene by the CRISPR/Cas9 system causes type I AT deficiency

Based on the results of a previous study[20], we injected fertilized zebrafish eggs with gRNA targeting Exon1 of the zebrafish *SERPINC1* gene, along with Cas9 nuclease. These fertilized eggs were cultured until 5 days post fertilization (dpf) and then subjected to partial genotyping. The results showed that these F0 fish were a genetic mosaic of the *SERPINC1* gene, presenting a variety of mutations (Supplementary Fig. 1). We subsequently reared F0 zebrafish to adulthood and crossed them with wild-type zebrafish to produce $zAT^{+/-}$ progeny. Direct sequencing analysis of these $zAT^{+/-}$ zebrafish revealed the deletion of five bases (ACTTA) and the heterozygous insertion of one base (C) (Fig. 1A). Consequently, the $zAT^{+/-}$ zebrafish represents a frameshift mutant harboring an early stop codon. This mutation results in a substantially altered structure of the mutant zAT protein, which is predicted to lack its native functional abilities and exhibit a significantly truncated polypeptide chain relative to the normal zAT protein. We successfully established $zAT^{-/-}$ zebrafish by crossing $zAT^{+/-}$ individuals. Native-PAGE analysis detected a 4-bp deletion in the *SERPINC1* gene on both chromosomes of the $zAT^{-/-}$ zebrafish (Fig. 1B; Supplementary Fig. 2). Relative expression levels of the *SERPINC1* gene in zebrafish at 7 dpf were 1.24 for $zAT^{+/+}$ and 1.14 for $zAT^{+/-}$, with no significant difference observed ($p = 0.37$; Fig. 1C). However, $zAT^{-/-}$ demonstrated a significantly reduced gene expression level of 0.90 compared to $zAT^{+/+}$ ($p = 0.048$; Fig. 1C). As the zebrafish were reared to adulthood, blood was collected and centrifuged to obtain plasma. Following separation by SDS-PAGE, the zAT protein was detected at approximately 50 kDa by western blot analysis using an anti-zAT antibody (Fig. 1D; Supplementary Fig. 3). This molecular weight is comparable with the predicted molecular weight of zAT (50.8 kDa). Quantitative analysis of the zAT protein revealed relative protein levels of 35% for $zAT^{+/-}$ and only 2% for $zAT^{-/-}$, in comparison to the 100% observed in $zAT^{+/+}$ (Fig. 1E). These findings demonstrate that the established mutant zebrafish exhibit markedly reduced AT expression, confirming the development of hereditary type I AT deficiency.

Survival rate of juvenile zebrafish with hereditary AT deficiency reduced due to thrombosis and fibrin production

The respective fluorescence image data and the corresponding sites of the juvenile zebrafish are summarized in Fig. 2A. To examine the impact of zAT deficiency on zebrafish development, we initially assessed survival rates up to 9 dpf. Compared to the $zAT^{+/+}$ cohort, survival rates were significantly reduced in both $zAT^{+/-}$ (88.24%, $p = 0.0012$) and $zAT^{-/-}$ zebrafish (88.16%, $p = 0.0013$) (Fig. 2B). However, there was no significant difference in survival rates between $zAT^{+/-}$ and $zAT^{-/-}$ zebrafish ($p = 0.257$). Next, to clarify the reasons underlying the reduced survival rates in the zAT mutants, we analyzed the blood flow in *Tg(gata1:dsRed)* zebrafish at 8 dpf. In $zAT^{+/+}$ zebrafish, there were no clots in the heart and red blood cells in the pectoral fin vessel (PFV) and posterior cardinal vein (PCV) flowed normally (Fig. 2C,D; Video 1, 2). In contrast, some zAT mutants exhibited thrombus formation in the heart, though they maintained the ability to pump blood (Fig. 2E; Video 3). We also observed zAT mutants exhibiting occlusion of the PFV or PCV, which prevented blood flow to downstream vessels (Fig. 2F,G; corresponding to Video 4 and 5, respectively). In the most severe cases, some zAT mutants were incapable of pumping blood throughout the body due to extensive occlusion of most blood vessels near the heart (Fig. 2H; Video 6). These severe occlusions typically led to the death of the affected zebrafish by the following day. In the zebrafish manifesting the symptoms depicted in Fig. 2H, fibrin deposition was observed in the vessels surrounding the heart by immunofluorescence staining using an anti-fibrin antibody (Fig. 2I). Fibrin is produced by the cleavage of fibrinogen by thrombin and stabilizes blood clots through polymerization and aggregation[21,22]. These results show that aberrant blood coagulation accompanied by fibrin deposition

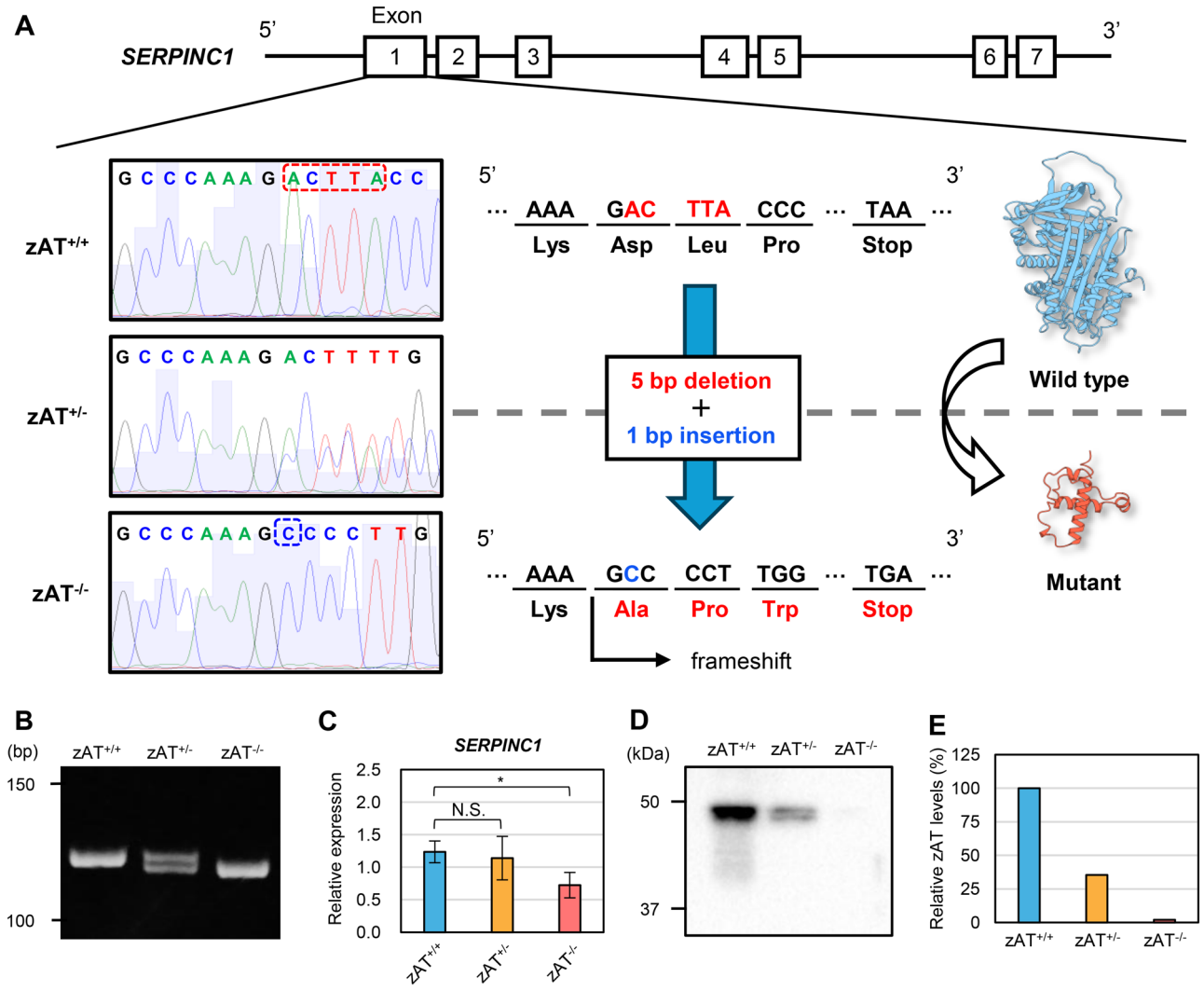

Fig. 1. Characterization of zAT mutant zebrafish demonstrating hereditary type I AT deficiency. (**A**) Sequencing analysis of exon 1 of the *SERPINC1* gene in wild-type and zAT mutant zebrafish revealed the deletion of five bases (ACTTA; shown by the red dotted line), and the insertion of a single base (C; shown by the blue dotted line). Ribbon models illustrate the structural differences between the wild-type (blue ribbon) and mutant (red ribbon) zAT proteins as predicted by ColabFold. (**B**) Genotyping of $zAT^{+/+}$, $zAT^{+/-}$, and $zAT^{-/-}$ was performed by detecting a four-base deletion by Native-PAGE. (**C**) *SERPINC1* mRNA levels showed no significant difference between $zAT^{+/+}$ and $zAT^{+/-}$ (N.S., not significant; $p = 0.37$; n = 3), but were significantly lower in $zAT^{-/-}$ compared to $zAT^{+/+}$ ($p < 0.05$; n = 3). (**D**, **E**) Detection and band quantification of zAT protein in zebrafish plasma by western blot analysis using an anti-zAT antibody.

leads to circulatory disturbance, markedly reducing the survival rates of zAT mutant zebrafish during the early developmental stages. The incidence of these thromboses is summarized in Fig. 2J.

Severe type I AT deficiency delays the development of intersegmental vessels in zebrafish embryos but does not affect overall angiogenesis

Intersegmental vessels (ISVs) begin to develop from the dorsal aorta at 24 h-post fertilization (hpf), before extending dorsoventrally. These vessels reach the dorsal lateral region and form dorsal longitudinal anastomotic vessels (DLAVs) by approximately 30 hpf[23,24]. Consequently, to study the development of ISVs on this developmental process, *Tg*(*fli1:GFP*)-type zebrafish embryos at 30 hpf were analyzed (Fig. 3A). In $zAT^{-/-}$ embryos, the percentage of ISVs that formed DLAVs (Completed ISV; red arrows) was significantly lower at 65.8%, compared to 82.0% in $zAT^{+/+}$ ($p = 0.0019$; Fig. 3B). In addition, the average length of ISVs was also significantly reduced in $zAT^{-/-}$ embryos, measuring 88.8 µm, compared to 95.3 µm in $zAT^{+/+}$ ($p = 0.027$; Fig. 3C). Conversely, no significant differences were observed in the angle between the ISV and the dorsal aorta and the distance between adjacent (Fig. 3D,E). These findings suggest that while severe AT deficiency delays the development of ISVs, the ultimate formation and spatial arrangement of these vessels remain normal. Indeed, observations of vascular structures in zebrafish at 5 dpf revealed no differences in vessel formation irrespective

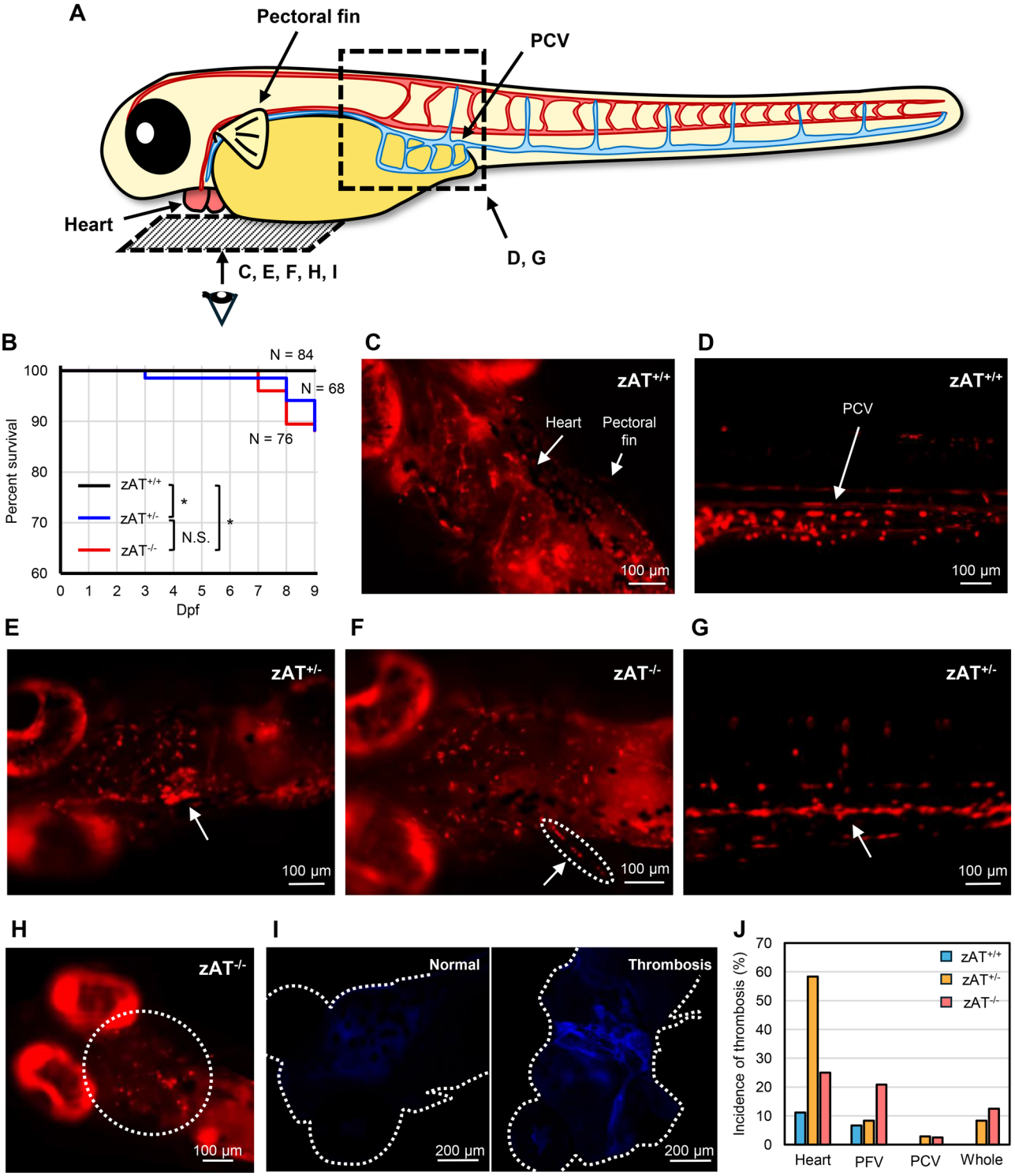

of AT deficiency status (Fig. 3F). In all studies in this section, zAT$^{+/+}$, zAT$^{+/-}$ and zAT$^{-/-}$ zebrafish were analyzed with N = 6, respectively.

Severely AT deficient juvenile zebrafish alter expression levels of coagulation- and fibrinolysis-related genes

While all AT$^{-/-}$ mice die at the fetal stage, approximately half of the zAT$^{-/-}$ zebrafish in the previous study survived up to 150 dpf[13,14]. Additionally, it was observed that zAT$^{-/-}$ zebrafish are capable of reproduction (data not shown). We therefore hypothesized that juvenile zebrafish possess mechanisms that mitigate the development of thrombosis.

To gain insight into the inhibition mechanism of thrombus formation in juvenile zebrafish, we performed transcriptome analysis using total RNA obtained from a whole fish to examine the gene expression profiles of zAT$^{-/-}$ compared with those of zAT$^{+/+}$. In this experiment, we used adult fish for RNA extraction because

◀**Fig. 2**. Survival curves and thrombosis sites of zAT mutants. (**A**) Illustration of a juvenile zebrafish. Arteries are shown in red and veins in blue. The dotted rectangular area and the alphabet correspond to the multipanel figures in Fig. 2. The locations of the heart, pectoral fin, and PCV are indicated by arrows. The positioning of the blood vessels and heart was based on previous studies by Lee et al.[45]. (**B**) Comparative survival rates between $zAT^{+/+}$ zebrafish and $zAT^{+/-}$ or $zAT^{-/-}$ zebrafish, illustrating survival differences across genotypes. The sample sizes are N = 84, 68, and 76 for $zAT^{+/+}$, $zAT^{+/-}$, and $zAT^{-/-}$ zebrafish, respectively. N.S., not significant; $^{*}p < 0.05$. The survival rates for $zAT^{+/+}$, $zAT^{+/-}$, and $zAT^{-/-}$ zebrafish on the 9dpf were 100%, 88.24%, 88.16%, respectively. (**C**, **D**) Fluorescent images of erythrocytes in $zAT^{+/+}$ zebrafish, focusing on the heart, pectoral fin vessel (PFV), and posterior cardinal vein (PCV). (**E**–**H**) Fluorescence imaging depicting thrombosis in zAT mutant zebrafish. Red fluorescence represents erythrocytes. White arrows or areas circled by white dotted lines indicate thrombus locations in the heart (**E**), pectoral fin (**F**), and PCV (**G**). An instance of a beating heart with restricted systemic blood flow is shown in (**H**). (**I**) Immunofluorescence staining of juvenile zebrafish displaying the same symptoms as in (**H**), using an anti-fibrin antibody, with blue fluorescence indicating fibrin. The zebrafish is outlined with a white dotted line. (**J**) Incidence of thrombosis in the heart, PFV, PCV, and systemic circulation corresponding to (**E**–**H**), respectively. Sample sizes for heart, PFV, and systemic are N = 45 for $zAT^{+/+}$ zebrafish, N = 12 for $zAT^{+/-}$ zebrafish, and N = 24 for $zAT^{-/-}$ zebrafish. The number of samples for PCV is N = 45 for $zAT^{+/+}$ zebrafish, N = 35 for $zAT^{+/-}$ zebrafish, and N = 40 for $zAT^{-/-}$ zebrafish.

the transcriptome analysis requires large amount of RNA. As a result, no expression changes were observed in 30,075 genes, but significant expression increases were observed in 1535 genes and decreases in 1126 genes. Interestingly, these analyses revealed remarkable upregulation of *PLG* and downregulation of *F5* among the blood coagulation factors. For confirmation and further understanding of expression alternations in $zAT^{-/-}$, we analyzed the expression levels of these genes and several related factors by RT-qPCR, in which we prepared total RNA from juvenile zebrafish. In agreement with the transcriptome analysis using adult fish, the expression levels of the *PLG* gene, which expresses plasminogen, the precursor protein of plasmin that is involved in thrombolysis, in $zAT^{+/-}$ and $zAT^{-/-}$ were significantly increased compared to $zAT^{+/+}$ ($p = 0.023$ and $p = 0.047$, respectively; Fig. 4A). Similarly, we investigated the gene expression levels of *F5*, and additionally we analyzed the gene expression levels of coagulation factor II (*F2*) and X (*F10*) using the same methods. Prothrombin, encoded by the *F2* gene, and coagulation factor X (FX), encoded by the *F10* gene, are serine proteases that are regulated by AT and play a central role in the cascade reaction for blood clot[25,26]. FX is activated by endogenous and exogenous tenase to form activated FX (FXa)[21,25], which binds to FV, encoded by the *F5* gene, and converts prothrombin into thrombin[27]. The findings showed that the gene expression level of the *F2* gene was significantly decreased in $zAT^{-/-}$ compared to $zAT^{+/+}$ ($p = 0.0033$; Fig. 4B), while those of the *F5* and *F10* genes were not significantly different between $zAT^{+/+}$ and $zAT^{+/-}$, nor between $zAT^{+/+}$ and $zAT^{-/-}$ (Fig. 4C,D). The expression analyses of the *F2* and *F5* genes showed different results from those of transcriptome analysis using adults. Also, the gene expressions of *PROS1* and *PROCA* genes, which encode the major anticoagulant factors protein S and protein C, were analyzed using same method described above. However, the expression levels of both genes in $zAT^{+/-}$ and $zAT^{-/-}$ were comparable to those in $zAT^{+/+}$, without significant differences (Fig. 4E,F). These results suggest that juvenile zebrafish possess adaptive mechanisms that mitigate thrombosis by reducing thrombin production in hypercoagulable states, and also by promoting thrombus lysis by increasing plasminogen production. In RT-qPCR analyses in this section, $zAT^{+/+}$, $zAT^{+/-}$ and $zAT^{-/-}$ zebrafish were analyzed with N = 3, respectively.

Discussion

To date, our understanding of the impact of severe hereditary AT deficiency on fetal development remains limited. There are documented cases of homozygous AT deficiency involving type II variants such as AT Toyama (p.Arg79Cys), p.Phe261Leu, and AT Budapest 3 (p.Leu131Phe)[28,29]. In a case specific to fetuses, a severe AT deficiency involving a type I variant, c.1154-14G > A, coupled with a compound heterozygous variant of AT Budapest 3, classified as type II, was reported to have died at 8 weeks gestation[12]. However, there have been no reports of patients with homozygous type I AT deficiency, suggesting that it is embryonically lethal in all cases. The precise mechanisms underlying this severe outcome have not yet been elucidated. In response, several animal models of AT deficiency have been proposed. For example, AT knockout mice have been reported to die at 16.5 days gestation due to fibrin deposition in the heart and liver[13]. Similarly, AT knockout zebrafish were observed to have fibrin deposition in the PCV when injected with FITC-labeled human fibrinogen[14]. Despite these insights, investigations into the mechanisms of thrombus formation in a living state remain scarce, and even fewer studies have successfully established animal models capable of spontaneously developing thrombosis.

In this study, we developed an animal model of type I AT deficiency by targeted mutagenesis of the zebrafish *SERPINC1* gene with the CRISPR/Cas9 system. Type I AT deficiency caused by frameshift mutations results in impaired intracellular trafficking of the AT protein, preventing its secretion into the blood and making it inaccessible to the coagulation cascade reactions that occur within blood vessels[30,31]. Presumably, nonsense-mediated mRNA decay (NMD) occurs in $zAT^{-/-}$ mutants due to the appearance of early stop codons, since the mRNA level in the *SERPINC1* gene was significantly reduced in the mutant. Initial physiological analyses have shown that NMD frequently occurs in zebrafish[32]. We also considered the possibility that the hypercoagulable state induced by type I AT deficiency might alter the expression levels of coagulation-related genes in juvenile zebrafish. To date, few studies have examined alterations in gene expression levels resulting from blood coagulation disorders. In an older example, the microarray analysis of gene expression after prothrombin knockdowns found out the alternation on two novel genes, *phlda3* and *sox21*[33]. More recently, mutagenesis of the *adcyap1b* gene, which encodes a pituitary adenylate cyclase-activating polypeptide in zebrafish, results in

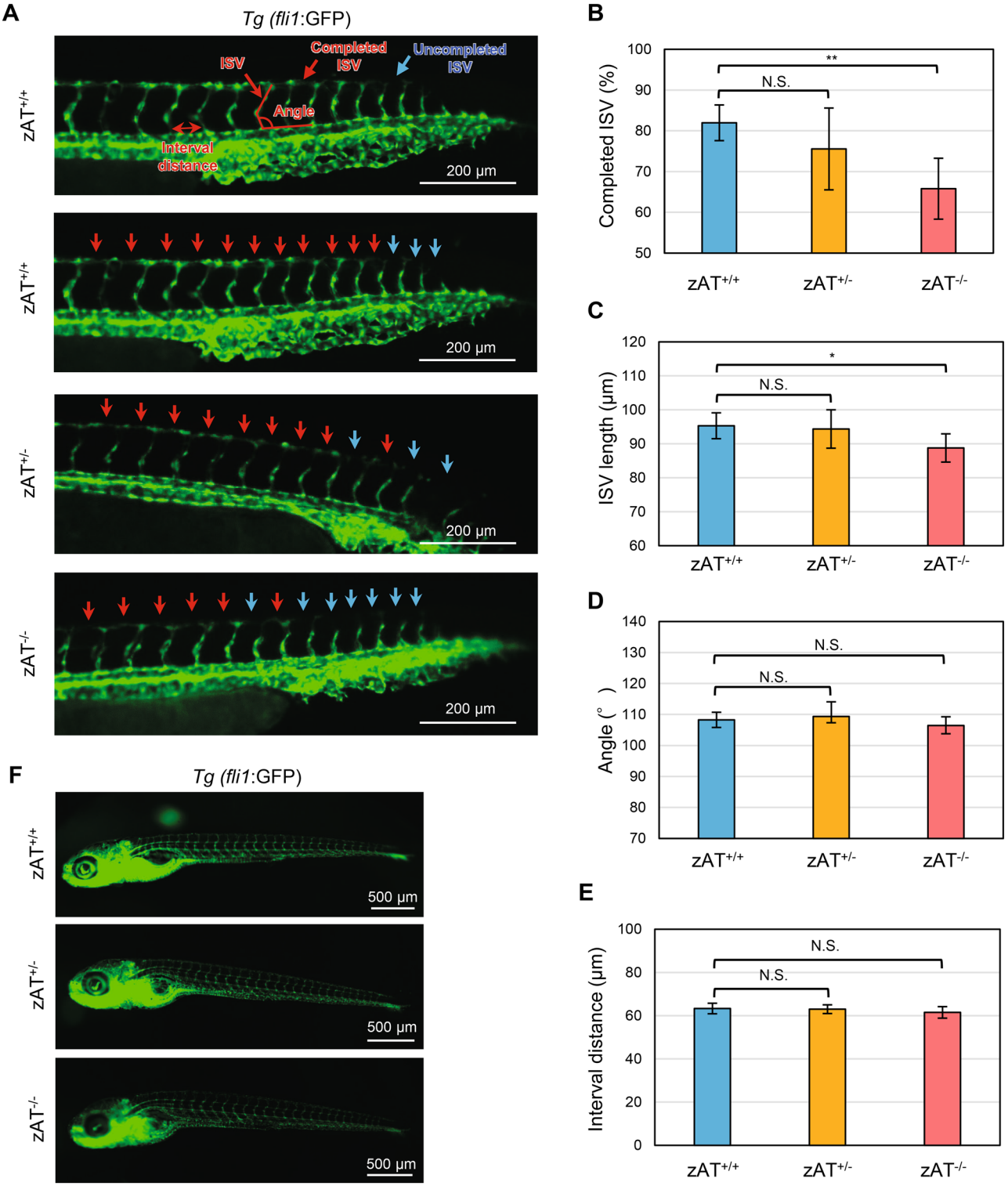

Fig. 3. Impact of severe zAT deficiency on vascular development. (**A**) Representative images of intersegmental vessel (ISV) development in zebrafish of different genotypes at 30 h post-fertilization (hpf). Red arrows indicate ISVs that have completed formation, while blue arrows indicate ISVs that have not yet completed formation. (**B**) Percentage of ISVs that have successfully completed formation across different genotypes. (**C**) Measurements of the length of ISVs in different genotypes. (**D**) Angle between each ISV and the dorsal aorta in different genotypes. (**E**) Distance between two adjacent ISVs in different genotypes. (**F**) Representative images at 5 days post-fertilization (dpf) showing overall vessel formation in different genotypes. Statistical significance is noted where applicable (N.S., not significant; $^{**}p < 0.01$; $^{*}p < 0.05$).

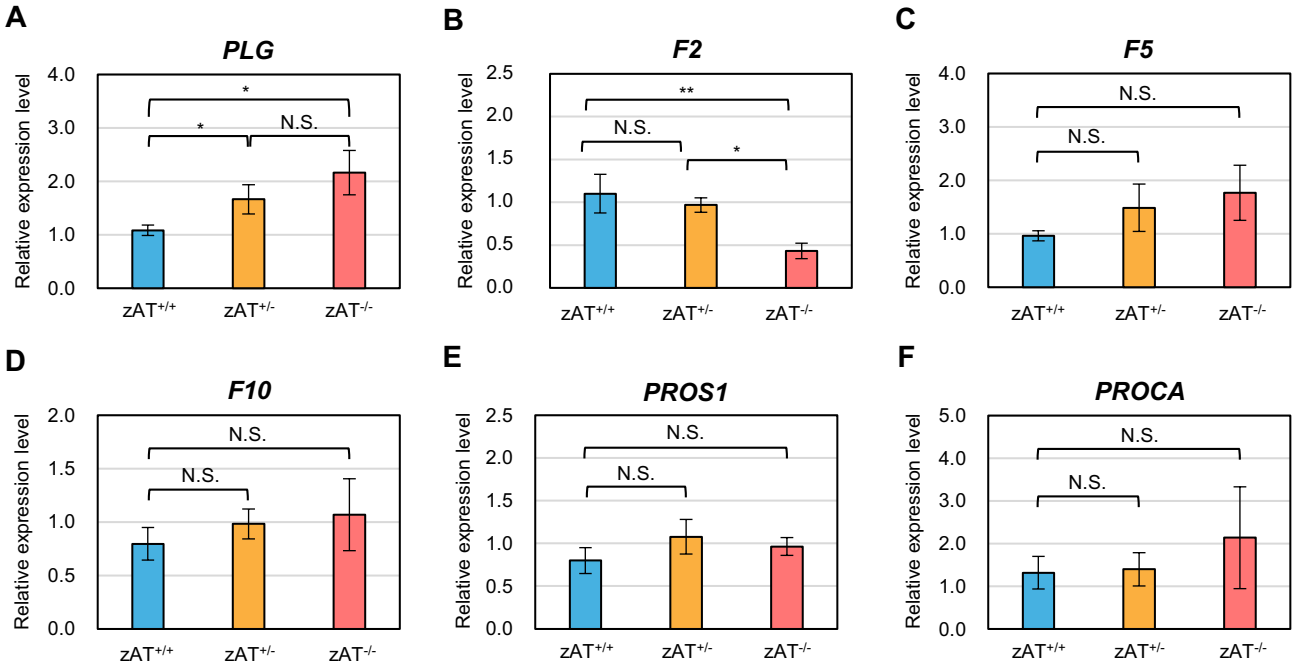

Fig. 4. Gene expression analysis in juvenile zebrafish at 7 days post-fertilization (dpf) by quantitative real-time PCR. Gene expression levels of protein S (**A**), protein C (**B**), plasminogen (**C**), prothrombin (**D**), coagulation factor V (**E**), and coagulation factor X (**F**) were compared between wild-type and mutant zebrafish. N.S., not significant; $^{**}p < 0.01$; $^{*}p < 0.05$.

bleeding symptoms as early as 24 hpf[34]. In contrast, RNA-Seq analysis and RT-PCR have shown a decrease in *PLG* expression and an increase in *F2* gene expression in this juvenile zebrafish model[34], which differs from the zAT mutant that results in a hypercoagulable state. Thus, it appears that the *PLG* and *F2* genes may play roles in monitoring the coagulation state of the blood and adjusting gene expression levels accordingly.

To our knowledge, the molecular mechanisms by which the AT gene directly regulates the expression of other genes have been largely unexplored. While we have demonstrated that AT gene deficiency reduces prothrombin expression, it remains unclear whether the AT gene itself directly regulates prothrombin expression. Additionally, AT gene deficiency may alter the expression levels of other factors, thereby indirectly regulating downstream genes. For example, increased thrombin levels may suppress prothrombin expression through a negative feedback mechanism. Alternatively, the coagulation state may be sensed independently of AT expression levels, leading to the activation of certain transcription factors and, consequently, the regulation of coagulation-related gene expression. This study serves as a starting point for further research into the regulatory mechanisms governing the expression of blood coagulation factors.

Live imaging of zAT mutant zebrafish revealed that they spontaneously develop diverse thrombophilia during early development, irrespective of their genotype. These symptoms include occlusion of small vessels, such as pectoral fin vessels, and systemic vascular occlusion accompanied by fibrin deposition, phenomena that have not been reported previously (Fig. 2E,G,H). Generally, the incidence of thrombosis in $zAT^{-/-}$ zebrafish was similar to, or higher than, that in $zAT^{+/-}$ zebrafish. However, intracardiac thrombosis was unexpectedly less frequent. Also, erythrocyte deposition in the heart was observed in approximately 10% of $zAT^{+/+}$ zebrafish, suggesting a mild thrombogenic propensity in zebrafish hearts during development. On the other hand, thrombus resolution in the hearts of $zAT^{-/-}$ zebrafish may be facilitated by suppression of the coagulation pathway, attributed to reduced *F2* gene expression and thrombin depletion in the hypercoagulable state.

Although several studies have reported that AT inhibits angiogenesis in contexts such as embryology and oncology, to our knowledge, no previous studies have specifically investigated the impact of AT knockout on vascular development[4–6]. Based on the anti-angiogenic properties of AT, we hypothesized that the zAT deficiency might result in rapid and abnormal blood vessel formation. However, the blood vessels in zAT-deficient zebrafish show delayed development only until 30 hpf and appear normal thereafter, and the survival of juvenile zebrafish is not adversely affected. While it has been established that AT overexpression can delay angiogenesis[5], it is possible that other factors may compensate for AT deficiency and regulate angiogenesis.

In addition to AT, there are extracellular serpin superfamily proteins harboring anti-angiogenic activity, which might compensate for the AT deficiency. For example, α1-antichymotrypsin (ACT) is present at a concentration of approximately 45 mg/dL in normal plasma, which is higher than that of AT, and increases in inflammatory states[35]. The previous study reported that ACT plays a protective role in eye diseases through its anti-angiogenic, anti-inflammatory, and antioxidant effects[36]. Another example is pigment epithelium-derived factor (PEDF), which also possesses anti-angiogenic activity[37,38], with PEDF concentrations in normal serum ranging approximately 9–14 mg/dL[39]. Recent studies suggested that PEDF-sEV, which encapsulates PEDF in

secretory extracellular vesicles as a drug carrier, is an effective nanotherapeutic agent for treating pathological vascularization in retinopathy[40]. While it is currently unclear whether these factors possess anti-angiogenic effects comparable to those of AT, they possibly play a compensatory role in regulating vascular formation.

In conclusion, we have successfully established a model of type I zAT deficiency through targeted mutagenesis of the zebrafish *SERPINC1* gene using the CRISPR/Cas9 system. Our in vivo studies revealed that zAT deficiency leads to various thrombotic conditions during development, although its impact on angiogenesis appears minimal. In addition, our findings suggest the existence of genetic pathways that may prevent coagulation and fibrinolytic activation systems, which are typically induced by the hypercoagulable state resulting from zAT deficiency. Further elucidation of the mechanisms underlying thrombus formation during development is expected to deepen our understanding of pathologies such as embryonic lethal blood coagulation disorders.

Materials and methods

Zebrafish strains and maintenance

The present study is approved by Kanazawa University Animal Experiment Committee. All the methods in this study were performed in accordance with the ARRIVE guidelines[41] and in accordance with Kanazawa University Safety Committee for Genetic Recombination Experiments. This study has been approved under reference number KINDAI 6-2666. Zebrafish strains, *Tg(fli1a:GFP)* and *Tg(gata1:dsRed)*, were maintained in a MEITO system (MEITOSUIEN Co. Ltd., Aichi, Japan) at 28 °C under a 14/10 h light/dark cycle. Zebrafish embryos were obtained by natural mating, and embryos and juvenile zebrafish were maintained in E3 medium (5 mM NaCl, 0.17 mM KCl, 0.33 mM $CaCl_2$, 0.33 mM $MgSO_4$) at 28 °C under a 14/10 h light/dark cycle. During functional analysis, juvenile zebrafish were maintained in 96-well plates in order to identify individuals.

CRISPR/Cas9-mediated editing of the *SERPINC1* gene in zebrafish

For CRISPR/Cas9-mediated mutagenesis, a guide RNA (gRNA) targeting exon 1 of the *SERPINC1* gene was designed based on the findings of a previous study[20]. Briefly, using double-stranded DNA as a template for gRNA, amplification was performed using target primer and backbone primers (Supplemental Table 1) by polymerase chain reaction (PCR) with PrimeSTAR Max DNA Polymerase (Takara Bio Inc., Shiga, Japan). PCR products were purified using a Wizard SV Gel and PCR Clean-Up System (Promega, Madison, WI, USA). These purified PCR products were then used to synthesize gRNA using a MEGAshortscript T7 Transcription Kit (Thermo Fisher Scientific, Waltham, MA, USA). Synthesized gRNA was purified with a mirVana miRNA Isolation Kit (Thermo Fisher Scientific). An injection mix comprising 3–5 nl (400 pg/nl Alt-R S.p.Cas9 Nuclease v3 (Integrated DNA Technologies, Inc., Coralville, IA, USA), 500 pg/nl gRNA, and 0.025% phenol red) was injected into 1-cell stage zebrafish embryos using a Nanoject III (Drummond Scientific Company, Broomall, PA, USA) with a glass needle.

Establishment of zAT$^{-/-}$ zebrafish and genotyping of mutant offspring

Adult zebrafish were anesthetized with 0.2 mg/ml tricaine, and a portion of their caudal fin was collected for genetic analysis. Juvenile zebrafish were humanely euthanized using 2 mg/ml tricaine. For genomic DNA extraction, samples were immersed in 50 µl of alkaline genome extraction buffer (25 mM NaOH, 0.2 mM EDTA) and heated at 95 °C for 1 h. Subsequently, the extraction solution was neutralized with 50 µl of 40 mM Tris–HCl (pH 8.2). If concurrent extraction of RNA and genomic DNA was required from adult or juvenile fish, then an ISOGEN extraction kit (Nippon Gene, Tokyo, Japan) was used following the manufacturer's instructions. Zebrafish embryos (F0) injected with the Cas9-gRNA complex were reared to adulthood and crossed with wild-type individuals. The F1 embryos were also reared to adulthood and used for obtaining genomic DNA. PCR targeting the mutated sites was performed using GoTaq Master Mixes (Promega), and heterozygous mutants (zAT$^{+/-}$) were identified by Native-PAGE and direct sequencing analysis (Fasmac, Kanagawa, Japan). The primer sequences are listed in Supplemental Table 2. Pairs of F1 adult zebrafish carrying identical mutations were crossed to obtain F2 zebrafish embryos. The genotypes of these embryos were determined by Native-PAGE and direct sequencing analysis. The structures of wild-type zAT and mutant zAT proteins derived from these zebrafish were predicted using ColabFold (https://colab.research.google.com/github/sokrypton/ColabFold/blob/main/AlphaFold2.ipynb)[42,43]. These models were visualized using the Cuemol software package (http://www.cuemol.org/ja/). For Native-PAGE analysis, a TBE polyacrylamide gel (15% polyacrylamide, 90 mM Tris, 80 mM boric acid, 20 mM EDTA) was run in TBE buffer (90 mM Tris, 80 mM boric acid, 20 mM EDTA) at 200 V for 140 min. The gel was stained with 0.01% Midori Green Xtra (Nippon Genetics, Tokyo, Japan) in TBE buffer for 15 min and gel images were captured using a FAS-Digi system (Nippon Genetics).

Preparation of anti-zAT antibody

Livers from adult zebrafish were harvested and total RNA was extracted using the previously described method (see "Establishment of zAT$^{-/-}$ zebrafish and genotyping of mutant offspring" section). The extracted total RNA was reverse transcribed using a High Capacity cDNA Reverse Transcription Kit (Thermo Fisher Scientific). Subsequently, PCR was conducted to amplify the zebrafish *SERPINC1* gene, excluding the signal peptide, using Tks Gflex DNA Polymerase (Takara Bio Inc.) and the primer set shown in Supplemental Table 3. The signal peptide sequence of zAT was predicted using the SignalP6.0 package (https://services.healthtech.dtu.dk/services/SignalP-6.0/) (Supplemental Table 4). The PCR products were subjected to 1% agarose gel electrophoresis, followed by purification using the Wizard SV Gel and PCR Clean-Up System (Promega). The purified gene was cloned into the pET21a vector at the *Nde*I and *Xho*I sites using Gibson Assembly Master Mix (New England Biolabs, Ipswich, MA, USA), and *E. coli* Rosetta (DE3) cells were transformed with the resulting plasmid. Cells were cultured until $A_{600} = 0.5$, and gene expression was induced by the addition of 0.1 mM isopropyl β-D-thiogalactoside (IPTG). The cells were cultured for 16 h at 20 °C and then centrifuged at 8340 g for 5 min

and resuspended in 50 mM Tris–HCl (pH 7.5), 150 mM NaCl, 10 mM imidazole, 5% glycerol 0.5%, and Triton-100. Following ultrasonic disruption, the cell lysate was centrifuged at 20,000 g for 15 min, and the pellet was collected. The zAT proteins, which had formed inclusion bodies, were then resuspended in 6 M guanidine hydrochloride, 20 mM Tris–HCl (pH 8.0), 300 mM NaCl, 10 mM imidazole, and solubilized by inverted mixing at 4 °C overnight. The solubilized product was then centrifuged at 20,000 g for 5 min and the supernatant was collected. The supernatant was applied to Ni–NTA Agarose (QIAGEN, Venlo, The Netherlands), and the resin was washed using wash buffer (50 mM Tris–HCl (pH 8.0), 300 mM NaCl, 10 mM imidazole). The zAT proteins were then eluted with elution buffer (8 M urea, 20 mM Tris–HCl (pH 8.0), 300 mM NaCl, 200 mM imidazole). The purified zAT was then concentrated to 2.25 mg/ml using an Amicon Ultra Centrifugal Filter, 10 kDa MWCO (Merck, Darmstadt, Germany). Finally, rabbits were immunized with the purified zAT to produce polyclonal anti-zAT antibodies at Protein Purification Industries Co., Ltd. (Gunma, Japan).

Plasma collection from zebrafish

We removed the tail of adult zebrafish that were humanely killed, as described above (Supplemental Fig. 4A). Zebrafish blood was collected by immersing the cut-end of the fish body in 40 µl of 0.1 M sodium citrate for 1 min. The collected blood was then centrifuged at 3000 g for 10 min to obtain plasma components (Supplemental Fig. 4B).

Western blot analysis

Zebrafish plasma was separated by SDS-PAGE on a 10% polyacrylamide gel and transferred onto a Trans-Blot Turbo Transfer Pack (Bio-Rad Laboratories, Inc., Hercules, CA, USA) using a Trans-Blot Turbo system (Bio-Rad Laboratories, Inc.). The membrane was blocked with 5% skim milk for 1 h, incubated with anti-zAT antibody, and reacted for 2 h at room temperature. The membrane was then washed and incubated for 1 h with Goat Anti-Rabbit IgG H&L (HRP) (Abcam plc., Cambridge, UK). After washing, the membrane was reacted with Clarity Western ECL Substrate (Bio-Rad Laboratories, Inc.) and chemiluminescence signals were detected using a ChemiDoc XRS + device (Bio-Rad Laboratories, Inc.). The detected bands were quantified using the Image Lab software package (Bio-Rad Laboratories, Inc.). The estimated molecular weight of zAT was calculated using the A Plasmid Editor (ApE) program (https://jorgensen.biology.utah.edu/wayned/ape/). Total plasma protein levels were measured using a Pierce BCA Protein Assay Kit (Thermo Fisher Scientific) to unify the amount of each protein that was subjected to SDS-PAGE.

Live fluorescence imaging

Blood vessels and red blood cells of juvenile zebrafish anesthetized with 0.1 mg/ml tricaine were observed under fluorescence using an Axio Zoom.V16 stereomicroscope (Carl Zeiss, Oberkochen, Germany). To facilitate the observation of blood vessels, the egg membrane was carefully removed using tweezers, ensuring no harm to the juvenile zebrafish. Images were analyzed using the ZEN3.3 (blue edition) software package, and movies were captured using OBS Stadio (https://obsproject.com/ja). After all images and videos were collected and analyzed, all samples were genotyped using the method described above (see "Establishment of zAT$^{-/-}$ zebrafish and genotyping of mutant offspring" section).

Whole-body immunofluorescent staining of juvenile zebrafish

Juvenile zebrafish at 7 days post-fertilization (dpf) were humanely euthanized as described above and fixed in 10% Formalin Neutral Buffer Solution (FUJIFILM, Tokyo, Japan) at room temperature. After fixation, zebrafish were washed in 1 × phosphate buffered saline (PBS) and treated with transparency and permeabilization using Sca/eCUBIC-1 Solution of the CUBIC Trial Kit (FUJIFILM). Wash again with PBS, an anti-fibrin antibody (Cat. No. MABS2155; Merck) diluted 500-fold in the working buffer (5% normal goat serum, 0.3% Triton X-100 in 1 × PBS) was reacted with the samples for 24 h at room temperature, followed by washing three times with 1 × PBS. Goat Anti-Mouse IgG H&L (Alexa Fluor 405; Abcam plc.) was then incubated at room temperature for 24 h, then washed three times with 1 × PBS for 30 min each. After transparency is performed again using Sca/eCUBIC-2 Solution of the CUBIC Trial Kit (FUJIFILM), fibrin fluorescence was observed using an All-in-One Microscope BZ-X810 (KEYENCE, Osaka, Japan).

Transcriptome analysis

zAT$^{+/+}$ and zAT$^{-/-}$ adult fish were euthanized and homogenized, respectively. Then, total RNA fractions were extracted using ISOGEN extraction kit (Nippon Gene, Tokyo, Japan) following the manufacturer's instructions. Transcriptome analysis was performed by the Strand-specific RNA-seq service by Azenta Life Sciences (Tokyo, Japan).

Quantitative real-time PCR (qRT-PCR)

Total RNA was extracted from a sample of five zebrafish with the same genotype at 7 dpf, and cDNA was prepared using a High Capacity cDNA Reverse Transcription Kit (Thermo Fisher Scientific). The qRT-PCR reaction mixture comprised 1 µl of the cDNA, 10 µl of KAPA SYBR Fast qPCR Master Mix (2 ×) ROX Low (Nippon Genetics), 0.4 µl of each of 10 µM qRT-PCR primer (Supplemental Table 5), and 8.2 µl of nuclease-free water. The qRT-PCR was performed for 40 cycles using a QuantStudio 3 real-time PCR system (Thermo Fisher Scientific). Ef1α primers were used for the control experiments (Supplemental Table 5). Data collection and analysis were conducted using the $\Delta\Delta C_T$ method.

Statistical analysis

Data are presented as the mean ± standard deviation (SD). The significance of differences between groups was evaluated using Student's *t*-test, with a significance level of $p < 0.05$. Survival curve comparisons were analyzed by log-rank testing performed with EZR software (Saitama Medical Center, Jichi Medical University, Saitama, Japan)[44].

Data availability

Data are available upon request from the corresponding author, Yuhei Araiso (araiso@staff.kanazawa-u.ac.jp). The mutant used in this study has been deposited in The Zebrafish Information Network (ZFIN) database (https://zfin.org/) under allele number kz101 and accession number ZDB-ALT-250124-4. Whole transcriptomic data of RNA-seq analysis have been deposited in NIH Sequence Read Archive (SRA) database as reference number PRJNA1261223 (https://www.ncbi.nlm.nih.gov/sra/).

Received: 17 December 2024; Accepted: 7 May 2025
Published online: 27 May 2025

References

1. Corral, J., de la Morena-Barrio, M. E. & Vicente, V. The genetics of antithrombin. *Thromb. Res.* **169**, 23–29 (2018).
2. Olson, S. T., Richard, B., Izaguirre, G., Schedin-Weiss, S. & Gettins, P. G. Molecular mechanism of antithrombin regulation of blood clotting proteinases. A paradigm for understanding proteinase regulation by serpin family protein proteinase inhibitors. *Biochimie* **92**, 1587–1596 (2010).
3. Rezaie, A. R. & Giri, H. Anticoagulant and signaling functions of antithrombin. *J. Thromb. Haemost.* **18**, 3142–3153 (2020).
4. O'Reilly, M. S., Pirie-Shepherd, S., Lane, W. S. & Folkman, J. Antiangiogenic activity of the cleaved conformation of the serpin antithrombin. *Science* **285**, 1926–1928 (1999).
5. Larsson, H. et al. A novel anti-angiogenic form of antithrombin with retained proteinase binding ability and heparin affinity. *J. Biol. Chem.* **276**(15), 11996–12002 (2001).
6. Larsson, H. et al. Antiangiogenic effects of latent antithrombin through perturbed cell-matrix interactions and apoptosis of endothelial cells. *Cancer Res.* **60**(23), 6723–6729 (2000).
7. Di Minno, M. N. D. et al. Natural anticoagulants deficiency and the risk of venous thromboembolism: A meta-analysis of observational studies. *Thromb. Res.* **135**, 923–932 (2015).
8. Middeldorp, S. Is thrombophilia testing useful?. *Hematol. Am. Soc. Hematol. Educ. Program.* **2011**, 150–155 (2011).
9. Patnaik, M. M. & Moll, S. I Inherited antithrombin deficiency: A review. *Haemophilia* **14**(6), 1229–1239 (2008).
10. Alhenc-Gelas, M. et al. Thrombotic risk according to SERPINC1 genotype in a large cohort of subjects with antithrombin inherited deficiency. *Thromb. Haemost.* **117**(6), 1040–1051 (2017).
11. QIAGEN Digital Insights. Human Gene Mutation Database (HGMD) Professional. Available at https://my.qiagendigitalinsights.com/bbp/view/hgmd/pro/start.php. Accessed 22 July 2024.
12. Bravo-Pérez, C. et al. Genotype–phenotype gradient of SERPINC1 variants in a single family reveals a severe compound antithrombin deficiency in a dead embryo. *Br. J. Haematol.* **191**(1), e32–e35 (2020).
13. Ishiguro, K. et al. Complete antithrombin deficiency in mice results in embryonic lethality. *J. Clin. Invest.* **106**(7), 873–878 (2000).
14. Liu, Y. et al. Targeted mutagenesis of zebrafish antithrombin III triggers disseminated intravascular coagulation and thrombosis, revealing insight into function. *Blood* **124**(1), 142–150 (2014).
15. Weyand, A. C. & Shavit, J. A. Zebrafish as a model system for the study of hemostasis and thrombosis. *Curr. Opin. Hematol.* **21**(5), 418–422 (2014).
16. Hu, Z. et al. Genome editing of factor X in zebrafish reveals unexpected tolerance of severe defects in the common pathway. *Blood* **130**(5), 666–676 (2017).
17. Vo, A. H., Swaroop, A., Liu, Y., Norris, Z. G. & Shavit, J. A. Loss of fibrinogen in zebrafish results in symptoms consistent with human hypofibrinogenemia. *PLoS ONE* **8**(9), e74682 (2013).
18. Stainier, D. Y. R. Zebrafish genetics and vertebrate heart formation. *Nat. Rev. Genet.* **2**, 39–48 (2001).
19. Tu, S. & Chi, N. C. Zebrafish models in cardiac development and congenital heart birth defects. *Differentiation* **84**(1), 4–16 (2012).
20. Wu, R. S. et al. A rapid method for directed gene knockout for screening in G0 zebrafish. *Dev. Cell.* **46**(1), 112-125.e4 (2018).
21. Ząbczyk, M., Ariëns, R. A. S. & Undas, A. Fibrin clot properties in cardiovascular disease: From basic mechanisms to clinical practice. *Cardiovasc. Res.* **119**(1), 94–111 (2023).
22. Litvinov, R. I., Pieters, M., de Lange-Loots, Z. & Weisel, J. W. Fibrinogen and fibrin. *Subcell Biochem.* **96**, 471–501 (2021).
23. Dai, L. et al. Nanoplastics exposure induces vascular malformation by interfering with the VEGFA/VEGFR pathway in zebrafish (Danio rerio). *Chemosphere* **312**(Pt 2), 137360 (2023).
24. Zhong, X. et al. Exposure to tris(1,3-dichloro-2-propyl) phosphate (TDCPP) induces vascular toxicity through Nrf2-VEGF pathway in zebrafish and human umbilical vein endothelial cells. *Environ. Pollut.* **247**, 293–301 (2019).
25. Camire, R. M. Blood coagulation factor X: Molecular biology, inherited disease, and engineered therapeutics. *J. Thromb. Thrombolysis.* **52**(2), 383–390 (2021).
26. Davie, E. W. & Kulman, J. D. An overview of the structure and function of thrombin. *Semin. Thromb. Hemost.* **32**, 3–15 (2006).
27. Hertzberg, M. Biochemistry of factor X. *Blood Rev.* **8**(1), 56–62 (1994).
28. Picard, V. et al. Antithrombin Phe229Leu: A new homozygous variant leading to spontaneous antithrombin polymerization in vivo associated with severe childhood thrombosis. *Blood* **102**(3), 919–925 (2003).
29. Kovac, M. et al. The influence of specific mutations in the AT gene (SERPINC1) on the type of pregnancy related complications. *Thromb. Res.* **173**, 12–19 (2019).
30. Imai, Y. et al. Identification and functional analysis of three novel genetic variants resulting in premature termination codons in three unrelated patients with hereditary antithrombin deficiency. *Int. J. Hematol.* **117**(4), 523–529 (2023).
31. Imai, Y. et al. Functional analysis of two abnormal antithrombin proteins with different intracellular kinetics. *Thromb. Res.* **230**, 18–26 (2023).
32. Wittkopp, N. et al. Nonsense-mediated mRNA decay effectors are essential for zebrafish embryonic development and survival. *Mol. Cell Biol.* **29**(13), 3517–3528 (2009).
33. Day, K. R. & Jagadeeswaran, P. Microarray analysis of prothrombin knockdown in zebrafish. *Blood Cells Mol. Dis.* **43**(2), 202–210 (2009).
34. Ma, X. et al. Developmental adcyap1b loss leads to hemorrhage, disrupted hemostasis, and a blood coagulation cascade in zebrafish. *J. Thromb. Haemost.* **22**(4), 951–964 (2024).
35. Ortega, L., Balboa, F. & González, L. alpha(1)-Antichymotrypsin deficiency associated with liver cirrhosis. *Pediatr. Int.* **52**(1), 147–149 (2010).

36. Zhou, T. et al. SERPINA3K protects against oxidative stress via modulating ROS generation/degradation and KEAP1-NRF2 pathway in the corneal epithelium. *Invest. Ophthalmol. Vis. Sci.* **53**(8), 5033–5043 (2012).
37. Dawson, D. W. et al. Pigment epithelium-derived factor: a potent inhibitor of angiogenesis. *Science* **285**(5425), 245–248 (1999).
38. Yamagishi, S. et al. Pigment epithelium-derived factor (PEDF): Its potential therapeutic implication in diabetic vascular complications. *Curr. Drug Targets.* **9**(11), 1025–1029 (2008).
39. Szentimrei, R. et al. Changes in serum pigment epithelium-derived factor levels after kidney transplantation in patients with end-stage renal disease. *Ren Fail.* **44**(1), 1649–1659 (2022).
40. Fan, J. R. et al. Enhanced therapeutic effect of PEDF-loaded mesenchymal stem cell-derived small extracellular vesicles against oxygen-induced retinopathy through increased stability and penetrability of PEDF. *J. Nanobiotechnol.* **21**(1), 327 (2023).
41. Perciedu Sert, N. et al. Reporting animal research: Explanation and elaboration for the ARRIVE guidelines 2.0. *PLoS Biol.* **18**(7), e3000411 (2020).
42. Jumper, J. et al. Highly accurate protein structure prediction with AlphaFold. *Nature* **596**, 583–589 (2021).
43. Mirdita, M. et al. ColabFold: Making protein folding accessible to all. *Nat. Methods.* **19**(6), 679–682 (2022).
44. Kanda, Y. Investigation of the freely available easy-to-use software "EZR" for medical statistics. *Bone Marrow Transpl.* **48**(3), 452–458 (2013).
45. Lee, S. J., Park, S. H., Chung, J. F., Choi, W. & Huh, H. K. Homocysteine-induced peripheral microcirculation dysfunction in zebrafish and its attenuation by L-arginine. *Oncotarget* **8**(35), 58264–58271 (2017).

Acknowledgements

We thank the members of the Morishita and Araiso labs for valuable discussion. We thank K. Takata for technical support.

Author contributions

Y.I. established the zAT$^{-/-}$ zebrafish line, performed most of the experiments, and wrote the manuscript. S.O. and S.K. performed visualization of fibrin deposition by immunostaining of zAT$^{-/-}$ zebrafish. T.N. assisted with establishing the zAT$^{-/-}$ zebrafish line. I.K. assisted with designing the zAT$^{-/-}$ zebrafish. K.S. assisted with zebrafish dissection and tissue extraction. E.M. and Y.A. supervised the research and wrote the paper. All of the authors discussed the results and reviewed the manuscript.

Funding

This project was supported by the JST FOREST program (JPMJFR200F) to Y.A. Y.A. was also supported by the Leading Initiative for Excellent Young Researchers, MEXT, Japan. This work was supported by JST SPRING (JPMJSP2135) to Y.I.

Declarations

Competing interests

The authors declare no competing interests.

Additional information

Supplementary Information The online version contains supplementary material available at https://doi.org/10.1038/s41598-025-01658-z.

Correspondence and requests for materials should be addressed to E.M. or Y.A.